Design criteria for stability in cable-in-conduit conductors*

L. Bottura, N. Mitchell and J.V. Minervini†

The NET Team, c/o Max Planck Institut für Plasmaphysik, Boltzmannstrasse 2, D-8046 Garching bei München, Germany
†Los Alamos National Laboratory, Los Alamos, NM 87545, USA

Stability is a key point in the design of large conductors for application in fusion machines such as NET or ITER. In the electromagnetically noisy environment characterizing the surroundings of a plasma, the superconductor should be stable against all expected heat deposition, including a.c. losses driven by plasma disruptions. Since all sources of thermal perturbations cannot be adequately identified, predicted or calculated, the design must allow for suitable margins. To ensure this, stability must be considered as a design criterion which is checked by means of analytical and numerical methods and later calibrated against experimental measurements of transient heat transfer and stability behaviour. In this the procedure developed at NET is described for the design and analysis of the stability margin of conductors for the toroidal and poloidal field coils. These methods are applied to the generation of stability curves and maps which are used to set operating limits for the 40 kA NET conductor. The design criteria and analytical methods can be appropriately modified for other conductors and coil applications.

Keywords: superconductors; stability; design criteria

In the new generation of tokamak designs (e.g. NET and ITER[1]), one of the most important and demanding components is the superconductor magnetic system. Large coils, with several metres of free bore, producing magnetic fields up to 13.5 T in pulsed mode, will have to be operated safely and reliably throughout the life of the machine. To achieve this challenging goal, the conductor must be designed to be able to operate stably in a magnetically noisy environment. In particular, plasma disruptions will provide the most severe transient energy input, with field change rates as high as 40 T s^{-1} on the toroidal field coils and 20 T s^{-1} on the poloidal field coils, over characteristic times of the order of 20–50 ms. The typical energy deposition due to a.c. will range between 100 and 150 mJ cm^{-3} of strand materials. Due to the large magnitude of the predicted energy inputs, the design of the conductor must be based from the start on the stability margin.

Stability in superconducting cables, in particular in forced-flow cooled superconductors for fusion application, has been extensively studied over the last 15 years. Both experiments[2–5] and calculations with complex one-dimensional models[6] seem to confirm the good stability properties of cable-in-conduit conductors (CICCs). This is in fact one of the driving reasons for the choice of the conductor type in NET. However extrapolation of the experimental measurements or the direct application of the numerical models to the design of the conductor is not easy, and in most cases is very time consuming. Therefore simplified models were developed for the design and analysis of the cables of NET. These methods, although simple, are very effective for preliminary design and use in iterative optimization. In fact they also prove relatively accurate in predicting the stability behaviour of superconductors[7].

Zero-dimensional model for stability of cable-in-conduit conductors

Description of the model

Here we shall concentrate on the stability behaviour of large CICCs subjected to an energy input over a long length, so that locally in the normal zone the temperature gradient (and the heat flux) along the conductor length can be neglected. Due to the short time-scale involved in the thermal transient and recovery process (from several milliseconds up to some tens of milliseconds) we can also neglect the mass fluxes out of the normal zone. The jacket is usually formed of low conductivity material (such as stainless steel) and its effect, together with the electrical insulation surrounding the cable space, is to form a very effective thermal barrier in the time-scales considered. Finally we neglect the temperature gradients in the strand and in the helium cross-sections. This assumption is justified for CICCs, where the strand dimensions are of the order of millimetres and

*Paper presented at the Symposium on Superconductor Stability, 13–15 November 1990, Yokohama, Japan

0011-2275/91/070510-06

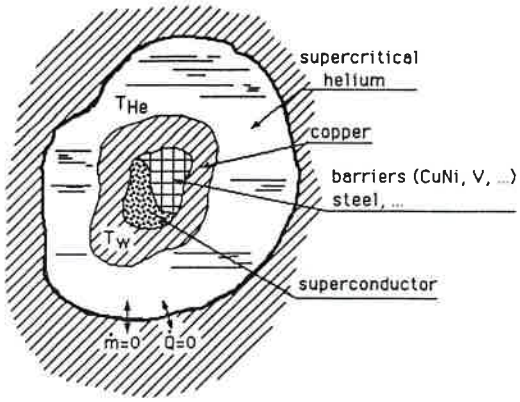

Figure 1 Schematic representation of the zero-dimensional model for stability calculations

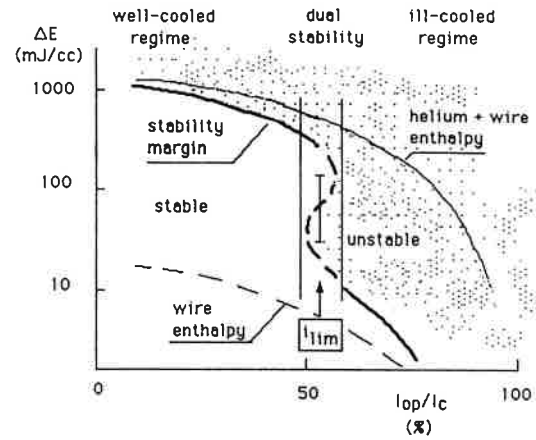

Figure 2 General behaviour of stability margin as a function of operating current. The units on the *y*-axis are arbitrarily set to indicate the order of magnitude of the stability margin

the turbulent mixing of the helium is very effective. The cable space in the normal zone is therefore an adiabatic closed system, which we can represent by an assembly of lumped heat capacities, as shown in *Figure 1*. In particular the heat capacities to be included in the model are those of the strand material (superconductor, copper, diffusion and resistive barriers in the strand) and of helium. For fast transients, in the millisecond range, the penetration depth of the heat diffusion wave in the conduit is very small (or the order of 0.3 mm in 10 ms for stainless steel). Therefore the heat capacity of the conduit (and obviously of the surrounding insulation) does not actively participate in the heat absorption.

According to the assumption of a closed system, the thermodynamic process in the helium takes place under constant density conditions. Therefore the correct measure of the heat capacity should be the specific heat at constant volume. In reality, however, the boundaries of the normal zone expand during the recovery process and the helium cools down at the end of the pressure excursion. This causes an apparent increase in the heat absorption capability of the helium[4] which we take into account by using the differences in enthalpy, rather than internal energy, at constant volume. The complete model is described by a coupled system of two ordinary differential equations in time, one for the temperature of the wires and one for that of helium. The coupling is represented by the heat transfer between the two. A thorough description of this model has been given in Reference 7, which should be referred to for more details.

General behaviour of the stability margin

With the previous model the problem of the stability of a superconductor reduces to a nonlinear heat balance of easy interpretation. As it has been shown experimentally[3,8] and in computer simulations[7,9] the stability curves as a function of the operating current in the cable show a rather universal behaviour, schematically shown in *Figure 2*. At low operating current the stability margin is very high, limited only by the total enthalpy available in the cable space (metal and helium) between the initial bath temperature, T_b, and the current sharing temperature, T_{cs}. When the current increases, the stability margin decreases uniformly because of the decrease of T_{cs} until a threshold value of the current is reached, sometimes called the limiting current[10].

Above the limiting current a dramatic fall in the stability margin can be observed (one to two orders of magnitude) until at the lowest limit the stability margin reaches the available enthalpy in the metal within the cable space between T_b and T_{cs}. Below the limiting current the heat removal from the strands to the helium is higher than the heat production rate by Joule heating, and the entire heat capacity of the helium can be accessed; we call this operation region the well-cooled regime. Above the limiting current the Joule heat production rate exceeds the heat removal capability to the helium and the only heat sink is represented by the conductor itself, excluding the helium. The heat capacity of the helium is larger by orders of magnitude than that of the materials in the strand and this explains the sudden fall in the stability margin. We call this operating region the ill-cooled regime. The transition between the well- and the ill-cooled regimes can be found by means of a power balance between Joule heat production and heat transfer to the helium[8-11]. The fraction of the critical current, i, at which the transition takes place is given by

$$i_{lim} = \left[\frac{A_{Cu}ph(T_c - T_b)}{\eta I_c^2}\right]^{1/2} \quad (1)$$

where: A_{Cu} is the copper area; p is the wetted perimeter; h is the heat transfer coefficient; T_c is the critical temperature and I_c is the critical current of the superconductor (both functions of the applied field); and η is the copper resistivity. Equation (1) was originally developed for steady state operation of bath cooled conductors[11]. We use it in transient conditions as an indicator of the direction of the power balance.

Finally, the actual stability margin always lies below the maximum available enthalpy (helium plus metal) in the well-cooled regime, while it is always above the minimum available enthalpy (metal only) in the ill-cooled regime. The reason is that for a transient of finite

duration there will always be a certain amount of Joule heat production in the well-cooled regime and heat transfer to the helium in the ill-cooled one. The difference between the maximum available enthalpy and the stability margin in the well-cooled regime is given by the Joule heat production, while in the ill-cooled regime the stability margin is above the minimum enthalpy available by the amount of heat transferred to the helium during the pulse. This is the basis for the simplified stability model illustrated in the next section.

Simplified zero-dimensional model

Following what has been shown in the previous section, it is possible to simplify further the model for the calculation of the stability margin so that no differential equations need to be solved. We clearly separate the two operation regimes, the well- and ill-cooled portions of the stability curve. Far away from the transition the stability margin will be limited by the helium and metal enthalpy available in the first regime and by the metal enthalpy and transient heat transfer to the helium in the second one. In particular, in the well-cooled regime we can write that the stability margin, ΔE, is approximately

$$\Delta E \approx \frac{1 - f_{cu} - f_{nc}}{f_{cu} + f_{nc}} \rho_{He} \Delta H_{He} + \rho_M \Delta H_M - \frac{f_{cu} + f_{nc}}{f_{cu}} \eta J_{op}^2 \tau_n \qquad (2)$$

where: f_{cu} and f_{nc} are the fraction of copper and non-copper materials in the cable space area; ρ_{He} and ρ_M are the density of the helium and wire (averaged over the strand materials); and ΔH_{He} and ΔH_M are the specific enthalpy differences between the operating and current sharing temperature for the helium and wire (again averaged over the strand materials). We exclude from the wire contribution the conduit and other materials outside the cable space for reasons discussed earlier (long thermal time constant). The last term represents the Joule heat contribution to the energy balance, where η is the electrical resistivity of copper, J_{op} is the cable space operating current density and, finally, τ_n is the time spent by the conductor in the normal state. This last term can be estimated as

$$\tau_n = \tau_p + \tau_r$$

where τ_p is the expected duration of the energy pulse and τ_r is the recovery time after the pulse has ended. Assuming constant material properties for the problem, the recovery time is proportional to the characteristic time constant of the heat transfer between the wires and the helium. We can assume, in particular

$$\tau_r \approx \frac{A_M \rho_M C_M}{ph}$$

where A_M is the total area of strands in the cable and the proportionality constant has been taken to be equal to one. In any case the weight of τ_r on τ_n will be small in the well-cooled regime for pulse times of the order of and above 10 ms because of the good heat transfer and the quick recovery after the end of the pulse (in times of the order of milliseconds). The above approximation to the stability margin holds as long as $i \leq i_{lim}$. Getting closer to i_{lim} the enthalpy availability decreases, owing to the decrease in T_{cs} and the distance between the curves of total enthalpy and the energy margin increases as the Joule heating term becomes larger with increasing operating current.

Above the transition, we approximate the energy margin in the following way

$$\Delta E \approx \rho_M \Delta H_M + \frac{p}{A_M} (T_{cs} - T_b) \int_0^{\tau_p} h \, dt \qquad (3)$$

The last term in (3) represents the total energy transferred from the strand to the helium under a constant temperature difference, with the strands being at the current sharing temperature. The heat transfer coefficient is strongly variable in the first millisecond of an energy pulse[6,12,13]. We restrict our attention to the first millisecond of the pulse, when h has its maximum value and most of the energy is transferred to the helium. In this range the heat transfer coefficient is dominated by the diffusion process and a good estimate is given by[6,8,14]

$$h = \left(\frac{\lambda_{He} \rho_{He} C_{He}}{\pi t} \right)^{1/2} \qquad (4)$$

where λ_{He} and C_{He} are the helium thermal conductivity and specific heat (at constant pressure), respectively. We can substitute this in the approximation of the energy margin to obtain

$$\Delta E \approx \rho_M \Delta H_M + 2 \frac{p}{A_M} (T_{cs} - T_0) \left(\frac{\tau_p \lambda_{He} \rho_{He} C_{He}}{\pi} \right)^{1/2} \qquad (5)$$

Also in this case an increase in i corresponds to a lower stability margin, because of the decrease in T_{cs} in both terms on the right-hand side of Equation (5). In addition, the difference between the stability margin and the enthalpy available in the metal becomes smaller at increasing values of i.

Stability based design guidelines

According to the zero-dimensional models discussed in the previous section it is possible to identify three critical aspects relevant to the stability of the cable: the heat transfer from the strands to the helium, the Joule heat production and the available heat capacity (or enthalpy) in the cable cross-section. A stability based design has to take into account and find an optimum balance among these three aspects, as discussed in detail here.

Heat transfer. A good heat transfer to the helium is desirable and is usually obtainable by choosing a small strand diameter. Here the heat transfer coefficient during the transient is the critical parameter of the model. In its expression are buried all the uncertainties con-

nected with the behaviour of the thermal boundary layer under changing flow conditions. The heat transfer coefficient varies in time during the pulse: it assumes very large values at the beginning of a pulse due to the heat diffusion into the existing boundary layer[6,12,13] (in excess of 5000 W m^{-2} K^{-1}), then decreases according to Equation (4), proportional to the square root of the inverse of time until, typically after a time of the order of 10 ms from the beginning of the pulse, the thermal boundary layer is fully developed and the heat transfer coefficient reaches the steady state limit, with values of the order of 500−1000 W m^{-2} K^{-1}. For use in the zero-dimensional model a reasonable space-averaged value has to be specified as a function of time[7]. A further averaging of h in time is needed for the calculation of the copper fraction in the conductor. Both processes introduce errors and approximations which add to the uncertainty of the actual local value of the heat transfer coefficient. Luckily, as it will be shown later, the choice of the conductor design is not extremely sensitive to the average value of h.

Joule heat production. As it has been shown earlier, the balance between Joule heat production and heat removal to the helium is responsible for the transition from the well-cooled to the ill-cooled regime of operation, the former with a much larger stability margin than the latter. It is of obvious advantage to try to design the cable so that it operates in the well-cooled regime. Once the cable space current density is fixed the parameter which is most easily changed is the copper fraction in the strand. Using Equation (1) it is possible to calculate the copper fraction necessary to operate in the well-cooled regime at a given cable space current density. We express the wetted perimeter of the cable, in terms of the total area of the strands in the cable space, as

$$p = \frac{4K_p(A_{cu} + A_{nc})}{d}$$

where: A_{cu} and A_{nc} are, respectively, the copper and non-copper (superconductor and barriers) area in the strands; d is the strand diameter; and K_p is a corrective factor (≤ 1) taking into account the degradation of the wetted perimeter due to interstrand contacts and enclosed area (typically ⅔ for a triplexed based conductor). Using the fraction of copper, f_{cu}, and non-copper, f_{nc}, in the cable space area and substituting in Equation (1), we obtain the following limitation on the cable space current density for operation in the well-cooled regime

$$J_{CS} \leq [f_{cu}(f_{cu} + f_{nc})]^{1/2}\left[\frac{4K_p h(T_c - T_b)}{\eta d}\right]^{1/2}$$

Once the operating cable space current density is specified, the above expression can be used to derive the minimum fraction of copper which is necessary to operate in the well-cooled regime

$$f_{cu} \geq \frac{1}{2} K_{cu}\left\{\left[f_{nc} + \frac{\eta d J_{CS}^2}{K_p h(T_c - T_b)}\right]^{1/2} - f_{nc}\right\} \qquad (6)$$

where K_{cu} is a safety factor (≥ 1) for the copper fraction computed. Note that in Equation (6) f_{cu} depends on f_{nc}. Another condition should be used to set the non-copper fraction, e.g. on the void fraction of the cable. Another possibility is to evaluate f_{cu} iteratively in an optimization loop (e.g. on the energy margin of the conductor). Due to the fact that both the Joule heat production and the wetted perimeter depend on f_{cu}, the dependence of Equation (6) on h is only through the ½ power, so that relatively large uncertainties in the value assumed for the heat transfer coefficient result in minor changes in the copper fraction. Therefore a reasonable (conservative) guess for the average h is generally sufficient. We use the steady state heat transfer coefficient computed by the Dittus−Boelter correlation, usually in the range 500−800 W m^{-2} K^{-1}.

Available heat capacity. It is well known that the helium heat capacity is two orders of magnitude higher than that of the composites in the strands for cable space void fractions of the order of 40% and in the temperature range of interest in the calculation of the stability margin ($T \leq 15$ K). Setting the copper fraction to the value given by Equation (6), this heat capacity will be fully available for stabilization. This is a must for a conductor subjected to the large disruption a.c. loss predicted for the NET/ITER coils: in the short timescale considered a conductor working in the ill-cooled regime would have access only to a limited fraction of the helium enthalpy and very little chance to remain stable. To maximize the stability margin, according to Equation (2), it is necessary to use the smallest possible f_{cu} since, for a given non-copper fraction, the helium content in the cable increases monotonically at decreasing values of f_{cu}. This means that for a given f_{nc} Equation (6) not only gives the minimum necessary f_{cu}, but also its optimal value to achieve the highest stability.

The three aspects considered above can be summarized in an easy two-step design procedure: 1, compute the necessary copper fraction for operation in the well-cooled regime from Equation (6); and 2, evaluate the stability margin using Equation (2) and compare it to the predicted perturbation. These two steps can be repeated iteratively to adjust the various parameters and the operating point. In fact, if one leaves the non-copper fraction free to change, it is possible to iterate on step 2 for various copper fractions satisfying 1 (and possibly on other limits such as coil protection during quench), to obtain a maximum stability margin at a fixed cable space current density or to maximize the operating current density for a fixed minimum stability margin (for example for system studies). Once the design is fixed, a global scan can be performed using the simplified zero-dimensional model presented here, while local checks can be done in more detail using the full zero-dimensional model[7] or even more complex one-dimensional models[6]. It is generally a matter of good policy to use a safety factor in step 2, e.g. assuming that the actual energy margin is only a fraction K_c (≤ 1) of the computed margin.

Example of application

Details will now be shown of the application of the

previous models to the design of a 40 kA CICC for application in the central solenoid of NET/ITER. The design goals on the conductor are set by the requirements on the inductive flux capability of the solenoid and by space limitations in the machine. Assuming, that the coil cross-section has a certain percentage of structural material to satisfy the design allowances on the stresses, the overall current density which was set by the two initial requirements can be converted to a cable space current density. With the specifications of NET/ITER the cable space operating current density to be achieved is 43.5 A mm^{-2} at a field of 13.5 T and 48.2 A mm^{-2} at 12.5 T. These two values correspond to operating currents of 36.1 and 40 kA, respectively, in an available cable space area of 830 mm^2.

Nb_3Sn is the only possible choice in the given magnetic field with the levels of disruption energy input that are anticipated. Therefore the values of critical current and temperature are given. The void fraction of the cable can be roughly fixed from a practical point of view to $\approx 40\%$ of the cable space: lower values would result in higher pressure drop and cabling damage, higher values in mechanical instability of the strands. The choice of the strand diameter allows some freedom, with usual production values ≈ 1 mm. As we want to achieve good thermal contact with the helium, thus reducing the necessary fraction of copper to operate in the well-cooled regime, we have selected a relatively small value of 0.85 mm. Assuming that the average heat transfer coefficient is 800 W m^{-2} K^{-1} (close to that given by the Dittus–Boelter correlation at the nominal flow conditions of 7.5 g s^{-1}) and that the operating temperature is 4.5 K, one can now compute the copper fraction necessary to ensure operation in the well-cooled regime. In this case, we have fixed the fraction of metal in the cable space to 60% and therefore no iteration is needed on Equation (6). Assuming that $K_p = \frac{2}{3}$ and taking a 25% safety factor on the copper fraction ($K_{cu} = 1.25$, corresponding to $\approx 10\%$ safety factor on the operating current), we obtain, for well-cooled operation at 13.5 T, a copper fraction of 34%. At 12.5 T the copper necessary to operate in the well-cooled regime is less because the larger critical temperature compensates the increase in the current. In fact with the copper fraction set by the limit at 13.5 T one could operate in the well-cooled regime at 12.5 T up to a cable space current density of 50 A mm^{-2}, corresponding to a conductor current of 41.5 kA (operation at this current is however restricted by structural considerations).

At this point the various cross-sections are fixed and the stability margin can be computed for the operational space of the coil. We have done this as a function of conductor current and magnetic field using the simplified model of Equations (2) and (5). The results of this analysis are presented in *Figure 3* for a heat pulse time constant of 10 ms (in the range of the typical time-scale of a plasma disruption). Also indicated on this figure are the design points, showing that a margin in excess of 500 mJ cm^{-3} of strand is available in any operating condition along the load line indicated by the arrows connecting the open circles in the figure. As the expected energy inputs are below 150 mJ cm^{-3} of strand, the coil should be stable.

A further check was performed using the more complete zero-dimensional model of Reference 7 at the two design points considered. The value of the stability margin computed at these points is given in *Table 1*, where it is also compared to the results of the simplified model. The two models appear to be in good agreement, although the simplified zero-dimensional model always seems optimistic with regard to its estimation of the margin. Again this can be compensated by the use of the safety factor, K_c, typically in the range 0.7–0.8.

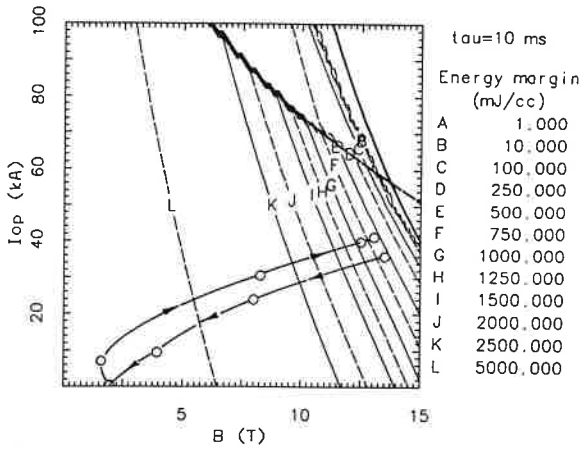

Figure 3 Map of stability margin in the operating plane of the NET central solenoid. Contours of stability are plotted as a function of operating current magnetic field in the coils. The plots show the critical current of the conductor (——) and the limiting current for operation in the well-cooled regime according to Equation (1) (– – –). The operating line of the coil is also indicated as an orientated trajectory (arrows) connecting some selected operating points (O)

Table 1 Comparison of results from the zero-dimensional stability model of Reference 7 (ΔE) and the simplified zero-dimensional model described here (ΔE_s) on the stability margin of the NET central solenoid for a 10 ms energy pulse. The deviation of ΔE_s relative to ΔE is also given

Magnetic field (T)	Operating current (kA)	ΔE (mJ cm^{-3})	ΔE_s (mJ cm^{-3})	Deviation (%)
12.5	40.0	635	898	40
13.5	36.1	513	589	15

Conclusions

Effective conductor design for superconducting magnets for fusion machines requires that high priority be given to achieving an adequate energy margin over possible sources of thermal disturbance. Among these is the heat generated from a.c. losses caused by plasma disruption. A simplified model for calculation of stability in forced-flow conductors has been developed. The combination of superconductor and copper is optimized so that the conductor operates at the upper end of the well-cooled portion of the stability curve. The model can be used for quick estimation of the stability margin and in optimization procedures, e.g. to maximize the operating current

density for a specified stability margin, given the strand diameter and helium fraction in the conductor, as well as the operating field and temperature. Here we have shown the application to the design of a stability optimized conductor for the central solenoid of the NET/ITER machine.

References

1 **Toschi, R.** ITER: design overview, paper IAEA-CN-53/F-1-2 presented at the 13th Int Conf on Plasma Physics and Controlled Nuclear Fusion Research (1990)

2 **Hoenig, M.O.** Cryostability experiments of force cooled superconductors *Proc IEEE Symp Eng Prob of Fusion Research* Knoxville, Tennessee, USA (1977) 780

3 **Miller, J.K., Lue, J.W. and Shen, S.S.** Nb_3Sn cable-in-conduit tests *Proc 8th Symp Eng Probs of Fusion Research* San Francisco, California, USA (1980) 1431

4 **Lue, J.W., Miller, J.K. and Dresner, L.** Stability of cable-in-conduit superconductors *J Appl Phys* (1980) **51**(1) 772

5 **Miller, J.R., Lue, J.W., Shen, S.S. and Dresner, L.** Stability measurements of a large Nb_3Sn force-cooled conductor *Adv Cryog Eng* (1980) **264** 654

6 **Arp, V.D.** Stability and thermal quenches in force-cooled superconducting cables *Proc 1980 Superconducting MHD Magnet Design Conf* MIT, USA (1980) 142

7 **Bottura, L. and Minervini, J.V.** Modelling of dual stability in a cable-in-conduit conductor, paper presented at 1990 Applied Superconductivity Conference, Snowmass Village, Colorado, USA

8 **Schmidt, C.** Stability of superconductors in rapidly changing fields *Cryogenics* (1990) **30** 501

9 **Schultz, J.H. and Minervini, J.V.** Sensitivity of energy margin and cost figures of internally cooled cable superconductors (ICCS) to parametric variations in conductor design *Proc 9th Int Conf Magnet Technology, MT-9* Zürich, Switzerland (1985) 643

10 **Dresner, L.** Parametric study of the stability margin of cable-in-conduit superconductors: theory *IEEE Trans Magn* (1981) **MAG-17** (1) 753

11 **Stekly, Z.J.J. and Zar, J.L.** Stable superconducting coils *IEEE Trans Nucl Sci* (1965) **12** 367

12 **Giarratano, P.J. and Steward, W.G.** Transient forced convection heat transfer to helium during a step in heat flux *J Heat Transfer ASME Trans* (1983) **105** 350

13 **Bloem, W.B.** Transient heat transfer to a forced flow of supercritical helium at 4.2 K *Cryogenics* (1986) **26** 300

14 **Holman, J.P.** *Heat Transfer* McGraw–Hill, New York, USA (1981)

Fusion Engineering and Design 20 (1993) 351–362
North-Holland

Stability, protection and ac loss of cable-in-conduit conductors – a designer's approach

L. Bottura

The NET Team, Max-Planck-Institut für Plasmaphysik, Boltzmannstrasse 2, W-8046 Garching, Germany

Stability margin, ac response (losses and current distribution) and protection issues (hot-spot temperature and maximum quench pressure) are the three primary aspects considered in the design of a superconducting magnet for application in an experimental fusion reactor. This paper reviews these three aspects in particular for cable-in-conduit conductors (CICCs). Their combination, together with the requirements on the performance of the magnet, determines a set of constraints to be satisfied at all operating points. This can be achieved only by means of compromises in the design, e.g. selecting the material fractions in the cable as a function of the specified margin and of the achievable current density. Here are presented some of the basic guidelines to be used for an effective design of a CICC, based in particular on simplified stability and hot-spot models.

1. Introduction

The conductor lay-out which is the first candidate for application in the next-generation fusion experiments based on magnetic confinement is the Cable-in-Conduit Conductor (CICC) [1]. What is the reason? There are several requirements typical of a fusion environment which have lead to this choice. First of all the magnets being designed are large. This implies that also the energy stored and the forces will be large. The magnets will be required to be stiff and mechanically stable, a condition which will be satisfied only with extensive bonding of conductors in the winding. This, in view of the relatively large power to be removed from the winding packs, implies the use of force-flow cooled conductors. Furthermore the necessity of dumping quickly the large stored energy will need a terminal voltage of the order of 20 kV, also requiring electrical stiffness, the necessity of good insulation among turns and therefore also calling for force-flow cooled conductors.

It is well known that force-flow cooled conductors have a limited stability margin [2], due to the limitations of the heat capacity available as heat sink during thermal perturbations. Stable operation of the magnet in an extremely *noisy* environment, characterized by large electromagnetic perturbations, will therefore require low ac losses and optimal stability performance. The first requirement can be fulfilled by CICCs by virtue of the fact that the strands are not soldered, and therefore a large contribution to the ac losses, the coupling loss in the cabling stages, can be kept to very low values in comparison to soldered cables. The optimal stability performance requires the best use of the available heat capacity, i.e. mainly the helium specific internal energy, which is achieved in CICCs through fine subdivision of the superconducting and stabilizer matrix in the helium channel.

Another advantage of CICCs over other possible geometries is the fact that the cable itself is rather soft, and therefore follows the deformation of the external jacket without large stress or strain accumulation [3]. This is extremely beneficial in the case that the strain sensitive Nb_3Sn is used as superconductor. Finally, CICCs are definitely easier to fabricate than soldered force-flow cooled conductors, because they only require repetitive cabling steps and a jacketing procedure. Both have been demonstrated as feasible and economically attractive for conductors of the size of interest in fusion application (typically up to 40 kA [4]).

Having justified the choice of the CICC as the most promising candidate for fusion application, it is necessary to examine the aspects which are left free to the designer and under which conditions the optimal design can be found. It is considered here that the

Correspondence to: Dr. L. Bottura, The NET Team, Max-Planck-Institut für Plasmaphysik, Boltzmannstrasse 2, W-8046 Garching, Germany.

optimal design condition corresponds to the achievement of the highest allowable current density in the winding pack of the magnet, once the operating and boundary conditions (mainly magnetic field and operating temperature) are set. This implies that the cross section of the magnet will be as small as possible and therefore that the cost will also be minimum (for a particular lay-out and material choice). With good approximation, the highest winding pack current density will be reached once the cable space current density is maximized (this is true if the cross section of structural material depends only on the cable space current density and the maximum field). Therefore, neglecting here the structural aspects, we are left just with the cable space of the CICC to be optimized. In this respect, the critical parameters which need to be set in the design of the CICC can be summarized in: superconducting material (e.g. NbTi or Nb_3Sn); critical current density and ac loss characteristics (mostly hysteresis losses); strand diameter; copper to non-copper ratio; strand coating, cabling pattern, twist pitches; void fraction; flow conditions (helium massflow, operating temperature and pressure). Their influence has to be studied mainly with regard to ac losses and current distribution effects, protection and stability of the magnet. In the detailed discussion of these aspects, we will identify the free parameters, their relations and the design constraints. The effort is to produce an optimized CICC, following the line of work of refs [5,6]. Some design guidelines and criteria will be given, and an optimization procedure will be presented. The *typical* CICC used as reference is shown in fig. 1. This conductor is formed by jacketing a bundle of cabled strands, and is the simplest form of CICC conceivable. Variants of this concept can be produced inserting extra copper strands for protection, cabling around a central hole or around perforated cooling tubes to decrease the pressure drop in the helium flow, using intermediate jackets either to protect the final cable stage or to create additional cooling channels, or, finally, inserting resistive barriers among the cabling stages to reduce the interstrand coupling. These variants are specifically adapted to different situations, but they do not substantially change the picture of the basic properties of the typical CICC.

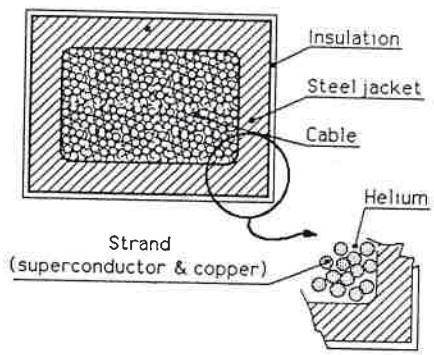

Fig. 1. Typical layout of a Cable-in-Conduit Conductor (CICC) used as reference in this work.

In this paper the fractions of components in the cable are referred to the cable space area A_{cs}, and are measured *normal to the conductor longitudinal axis*. For copper, non-copper (i.e. superconductor, barriers, etc.), helium and jacket the material fractions are defined respectively as:

$$f_{cs} = \frac{A_{cu}}{A_{cs}}, \quad f_{nc} = \frac{A_{nc}}{A_{cs}}, \quad f_{he} = \frac{A_{he}}{A_{cs}}, \quad f_{ss} = \frac{A_{ss}}{A_{cs}}.$$

The cross sections of copper and non-copper material measured *normal to the strand* are smaller than those used above because of the effect of the cabling angle. Indicating with θ the average cabling angle we have that the copper and non-copper cross sections normal to the strand are related to the cross sections normal to the conductor and to the cosine of the twist angle by the relations:

$$A_{cu}^{st} = A_{cu} \cos(\theta), \tag{1}$$

$$A_{nc}^{st} = A_{nc} \cos(\theta). \tag{2}$$

Note that with this assumption we have that $f_{cu} + f_{nc} + f_{he} = 1$ while f_{ss} can assume any value. Operating conditions of cable space current density, temperature and magnetic field (flux density) will be indicated with J_{op}, T_{op} and B_{op} respectively. Finally, it is useful to give here some relations, to be used later on, between the wetted perimeter w_p, the hydraulic diameter D_h, the strand diameter d and the material cross sections and fractions. We can assume with good approximation, due to the large number of strands, that the wetted perimeter of the conduit is negligible so that both wetted perimeter and the hydraulic diameter of the conductor are governed by the total strand surface. Therefore we have that:

$$w_p = K_p N \pi d = 4 K_p \frac{(A_{cu} + A_{nc})}{d}, \tag{3}$$

and that:

$$D_h = \frac{4 A_{he}}{w_p} = \frac{d}{K_p} \frac{f_{he}}{f_{cu} + f_{nc}}, \tag{4}$$

where the factor K_p, smaller than one, takes into account the reduction of the wetted surface due to interstrand contacts and dead volumes in the cable, and N is the number of strands in the cable. For use in calculation of heat transfer to the helium, the wetted perimeter must be measured on a circumference normal to the strand. We define therefore a *strand* wetted perimeter as:

$$w_p^{st} = w_p \cos(\theta). \tag{5}$$

2. The ac losses

In the configuration considered for a CICC the ac loss is mainly due to the following three mechanisms:

(1) hysteresis in the superconducting filaments, or, possibly, in bundles of bridged filaments within one strand,
(2) coupling losses within one strand and in the cabling stages,
(3) eddy current losses in the normal conducting components such as the conductor jacket.

Let us examine the characteristic behavior and magnitude of each of them in relation to the specific features of CICCs.

2.1. Hysteresis loss

For this loss component there is evidence that, apart from geometrical effects due to the twisting angle of the strands, there is little or no difference between the behavior of the CICC and the single strand [7]. Therefore the extensive analytical and experimental work (but also the fundamental difficulties) in the determination of the hysteresis loss in multifilamentary composites translate directly in the analysis of the whole cable [8–10]. We found the use of the effective filament diameter D_{eff} and its product with the critical current density J_c extremely useful to characterize the hysteresis loss of one strand [7,11]. Note that this does not imply the assumption of full penetration of the superconductor, although this is often the case for medium- to high-field applications, because both hysteresis losses and penetration field scale with the product $J_c D_{eff}$. The effective filament diameter D_{eff} is used as a fitting parameter to reproduce the hysteresis loss behavior of the strand and could be variable with the magnetic field. In general, however, there is a good correlation between the effective and geometric diameter of the superconducting filaments or, more often for Nb_3Sn, superconducting filaments bundles.

Although both the critical current density and the hysteresis loss of the strand are design parameters, they are correlated in the manufacturing of the superconducting strand and depend strongly on the superconductor chosen. In this respect it can be a complex matter to introduce them consistently in an optimization procedure. On the basis of the achievable production standards for the chosen material we take only one of them, the critical current density, as independent specification on the strand performance. The effective filament diameter, or directly the hysteresis loss for a specified field sweep, is set as an objective (to be verified experimentally) on the basis of the specification of J_c.

An idea of the importance of the hysteresis loss in fusion magnets is given by the fact that, with the present status of development of strand manufacturing technology, hysteresis is the dominating energy input (75% and up) for a typical, high performance, Nb_3Sn based CICC, operating at fields in the 10 T range and producing field sweeps of the order of 20 T in the coil bore, over a typical time scale of the order of tens of seconds.

2.2. Coupling loss

The geometry of the cable in a CICC can be extremely complex. Coupling current paths can close within a strand but also within each cabling stage, through the strand contacts. It is indeed very difficult to predict the behavior of a particular CICC with respect to the coupling loss, especially in the highest cabling stages. The basic unknown parameters, influencing the total loss, are the geometry of the contacts among strands and the contact resistances. The geometry of the contact is, in first approximation, set by the cabling and is therefore fixed once an overall conductor size and configuration are decided. The increase of the contact resistance by means of resistive coating of the strand surface prior to cabling is an effective way to reduce the coupling loss in the higher cabling stages. However, experience has shown that the use of too high contact resistances can be detrimental for the ac behavior of the cable, as this prevents the correct current sharing during fast transients [12,13]. The logical design guideline, to use an intermediate value to achieve good current transfer properties and acceptable losses, is difficult to quantify, as for both effects we lack satisfactory analytical models. In addition, at the moment, we also lack the technological capability

of controlling the contact resistances between strands during the manufacturing of the cable, because the value of the resistance depends on too many unknown parameters (e.g. the contact surface, its physical and chemical status, the acting pressure).

In view of these difficulties, experimental measurements must be used to qualify and characterize the coupling loss behavior of the full size cable [7,14]. Experiments have shown that the dominating coupling loss component is associated with the changes in magnetic field *transverse* to the conductor axis and that this component has an ohmic behavior. In particular conditions, changes of the magnetic field parallel to the conductor can cause an hysteretic behavior, often called *parallel* coupling loss [15]. This loss component is even more difficult to characterize, but it seems that its magnitude should be small compared to the other contributions for typical applications in fusion magnets (e.g. in the toroidal coils of a Tokamak). It is to be remembered that because of the twisting angle a component of the field parallel to the conductor axis acts transversely on the strands and cable stages, thus producing transverse coupling losses and further complicating the picture.

Based on the analytical expression of the coupling loss in a twisted multifilamentary composite [10,16], it is possible to characterize the transverse coupling loss in a cable through a geometrical factor n and a coupling time constant τ_c derived from the experimental measurements, so that the instantaneous power dissipated, in the low-frequency approximation, is given by:

$$P_c = \frac{n\tau_c}{\mu_0}\dot{B}^2. \tag{6}$$

The product $n\tau_c$ can be used as a figure of merit for the coupling loss of the different cabling substages up to the final cable stage. A typical example is shown in fig. 2, where the coupling loss power for a 40 kA prototype conductor has been measured as a function of frequency [7]. The global behavior of the cable in the whole frequency domain is more complex than above eq. (6) could explain. The effect of several time constants, for 5 substages plus the basic strand, could be visible in the experimental curves if one would measure at higher frequency. What is interesting, however, is just the low-frequency portion of the curves, which can be fitted to give the desired value of $n\tau_c$. Note, finally, that different curves are obtained depending on the orientation of the field, due to the effect of the aspect ratio of the cable [17]. This gives different coupling time constants and shape factors on

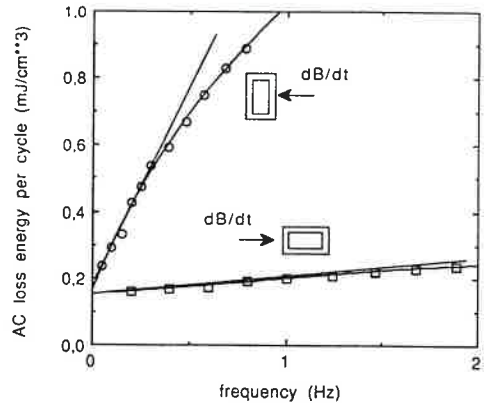

Fig. 2. Total ac loss energy per unit volume of strand and cycle generated by a field change with sinusoidal wave form in direction transverse to the conductor. The energy is plotted as a function of the wave frequency. Measurements performed on a 40 kA prototype conductor for NET (data from ref. [7]). The two curves refer to different orientation of the magnetic field with respect to the sides of the conductor. The linearization at low frequency (tangent at $f = 0$) is also shown.

the two sides of a rectangular cable. Two different values of $n\tau_c$ must be derived and used in the calculation of the losses.

The value of $n\tau_c$ from measurements can also give an indication of the current transfer properties of the cable. In analogy to the single strand time constant, the cable time constant is proportional to the inverse of the transverse resistivity of the bundle and to the square of the twist pitch. Owing to the twist pitch increase which is necessary for cabling the higher cable stages, a requirement on the transverse resistivity among strands can be translated in a specification on the relative increase of the coupling time constant in going to higher cable stages. For the moment, with lacking satisfactory models, we can tentatively assume that an increase of τ_c proportional to the square of the twist pitch should be satisfactory to maintain the transverse resistivity in the bundle to approximately constant values. Future experiments will be needed to show whether ensuring that the transverse resistivity is the same in all substages, up to the final cable, is a much too tight requirement. In this assumption the coupling loss is dominated by the contribution of the last cable stage.

As it is the case for the hysteresis losses, the value of the coupling loss of the last cable stage, or its figure of merit $n\tau_c$, is in effect an output of the cable manufacturing rather than an input parameter. In fact it can

only be specified as a design objective, whose achievement need to be demonstrated by means of experimental measurements.

To give an order of magnitude for the coupling loss contribution to the total ac loss in a large size fusion experiment, coupling losses in a 40 kA conductor will be of significant magnitude only during the fast electromagnetic transients involved in the induction of the initial plasma current or during plasma disruptions, when they actually dominate the energy input. On average they will typically amount to less than 25% of the total ac loss in the magnet.

2.3. Eddy currents

Eddy current losses in large size CICC are usually negligible, at least two orders of magnitude lower than the two components discussed in the previous sections, hysteresis and coupling. A pity, as they are also the easiest to treat. Many expressions, more or less approximated, are given in the literature for different geometries of the conducting structure and of the excitation field.

It is now easy to understand why the ac loss behavior is not usually taken as an optimization parameter, because it depends too strongly on the manufacturing details of the CICC. It is rather used to give design requirements on the cable operation and stability. The requirements are determined through the figures of merit and the field change patterns. The effective filament diameter, for the hysteresis losses, influences the steady state heating power in the magnet and, therefore, the operating conditions for the helium flow (massflow, temperature and pressure). The effective coupling time constant gives one of the contributions to the transient energy inputs to be considered for stability, usually the dominating one in large fusion experiments. Both, D_{eff} and $n\tau_{\mathrm{c}}$, are taken here as tentatively set to *reasonable* values and updated as a function of the experimental measurements.

3. Protection

A quench in a magnet for fusion application has to be regarded as a rare event, so that the magnet availability does not impact on the overall availability of the experimental device. Nevertheless, magnets can quench. With the large energy stored into fusion magnets it is not a surprise that protection is a fundamental issue both when the magnet is regularly dumped onto an external resistance and also in the case of a failure (switching failure, coil short, arcs). The CICC concept, as all other force-flow cooled conductors, has only a limited heat capacity available to withstand the temperature transients during a quench. Therefore the coil needs to be discharged by dumping the current quickly enough to prevent the local temperature of the cable and the local pressure in the helium to exceed specified limits.

The first limit, the hot-spot temperature, is usually set for CICCs between 100 and 150 K. Below this value the temperature gradient causes differential expansion which is negligible and therefore there is no need to perform detailed temperature and stress analyses of the winding pack to check that the thermal stresses are acceptable. To ensure that the hot-spot temperature is not exceeded, an adiabatic heat balance equating the energy deposited into the quench resistance to the heat capacity locally available is adequate [10]. In the heat balance all heat capacities should be taken into account, in particular the conductor jacket which gives a considerable contribution (of the order of 50% for a 40 kA conductor). This, in fact, might seem to be an optimistic treatment, as during a quench a substantial temperature gradient can develop among strands, helium and jacket. However, as the temperature gradient is driven by the Joule heating, which goes to zero at the end of the dump, the final temperature of all components in the cable will be approximately the same. Finally, the influence of the neighboring conductors in the winding pack can be neglected because of two reasons. First of all each conductor is insulated electrically from the neighboring ones, and therefore also thermally, to a very high degree. Then, the energy released locally during a dump is much higher than the stability margin of a conductor. This implies that a loss of a small fraction of the Joule heating of the conductor will propagate the quench transversely, causing also the neighboring conductors to become normal and therefore decreasing the transverse temperature gradients in the winding.

The adiabatic energy balance can be written in analytic form involving the cable temperature T (assumed uniform) as a function of time t:

$$\sum_i (A_i \rho_i C_i) \frac{\mathrm{d}T}{\mathrm{d}t} = \frac{\eta (J_{\mathrm{op}} A_{\mathrm{cs}})^2}{\cos(\theta)^2 A_{\mathrm{cu}}}, \tag{7}$$

where the index i has been used to indicate the contribution of a particular component (i = cu, nc, he, ss), ρ_i is the material density, C_i the specific heat and η is the copper resistivity. Introducing the material fractions f_i

and defining an average heat capacity in the cable space as:

$$\langle \rho C \rangle = \frac{\sum_i (f_i \rho_i C_i)}{\sum_i (f_i)}, \tag{8}$$

we can define the following integral γ as a *material* property for the cable (depending in reality also on the cable composition):

$$\gamma = \int_{T_{op}}^{T_{max}} \frac{\langle \rho C \rangle}{\eta} \mathrm{d}T. \tag{9}$$

Manipulating eq. (7) and assuming an exponential current dump with time constant τ_d we can derive a limit on the maximum allowable cable space current density for a given cable configuration:

$$J_{op} \le \cos(\theta) \sqrt{\frac{\gamma}{\tau_d/2} f_{cu} \sum_i (f_i)}. \tag{10}$$

The contribution of the helium to the total heat capacity between the operating temperature and the maximum allowed temperature, of the order of 150 K, is usually very small compared to the heat capacity of the solid materials (less than 10% for a void fraction of 40%). For simplicity, the helium can be neglected. Finally, if we make the further conservative assumption that the jacket does not contribute to the total heat capacity, eq. (10) simplifies:

$$J_{op} \le \cos(\theta) \sqrt{\frac{\gamma_{cu}}{\tau_d/2} f_{cu}(f_{cu} + f_{nc})}, \tag{11}$$

where only copper and non-copper fractions appear, and the integral γ can be referred to copper only because the heat capacity for the non-copper materials (e.g. bronze) is usually very similar to that of copper. Equation (11) is conservative, but has the advantage, compared to eq. (10), to require only the fractions of materials in the cable space, the real objects of the optimization.

The limit on quench pressure has to be set based on the stress limit of the conduit. Typical values for a 40 kA conductor can range, depending on the dimensions and the wall thickness of the jacket, between 100 and 300 bar. A good expression for the hot spot pressure during a quench is not available in closed analytical form. The reason is that the pressure depends on the evolution of the normal zone and therefore its study cannot be reduced to a local analysis. The expression for the maximum pressure p_{max} given by Dresner [18,19]:

$$p_{max} = 0.65 f^{0.36} \left(\frac{L^3 \dot{Q}_{he}^2}{D_h} \right)^{0.36}, \tag{12}$$

where f is the friction factor of the flow, L the flow length and $\dot{Q}_{he}^2$ is the joule heat production referred to the helium volume, is only valid for a whole conductor length normal under constant heat generation. It produces results which are largely over-estimated in common cases, when only a portion of the flow path is normal and the current is dumped. It can be used for preliminary, conservative dimensioning of a conductor, keeping in mind that in reality only a computer simulation of the helium expulsion will give realistic answers. Using algebraic manipulation of eq. (12), we can write the maximum allowable operating cable space current density in terms of the maximum acceptable quench pressure in the conduit:

$$J_{op} \le \cos(\theta) \left(\frac{p_{max}}{0.65} \right)^{0.69} \times \left(\frac{d}{K_p f L^3 \eta^2} \frac{f_{cu}^2 (1 - f_{cu} - f_{nc})^3}{f_{cu} + f_{nc}} \right)^{0.25}, \tag{13}$$

where the hydraulic diameter D_h in eq. (12) has been expressed in terms of strand diameter d and material fractions using eq. (4). A way to overcome, at least partially, the large safety margin in the above expression could be to use the expected final normal length in the pancake instead of the total pancake length L, e.g. one or several turns.

4. Stability

The ac losses, cable movements, releases of mechanical energy through friction and cracking, and nuclear processes are some of the normal operational and accidental energy inputs which need to be absorbed, without loss of stability, by the CICC on time scales in the range of 1 to 100 ms. In a fusion experiment the order of magnitude of these inputs can add up to some 100 to 200 mJ/cm^3 of strand for a 40 kA conductor, and is usually dominated by the energy deposition due to the coupling loss in fast electromagnetic transients (e.g. plasma disruptions). It is easy to verify that this amount of energy is well above – typically a factor 10 – the heat absorbing capability of the solid materials in

the cable space (the jacket and other external components are not affected during fast transients due to low thermal diffusion). The solution to this stability problem is the effective use of the heat capacity of the helium surrounding the strands. The heat capacity stored in the helium in a temperature margin of 2 K is of the order of 1500 mJ/cm^3 of strand (at 40% void fraction), therefore it is beneficial and indeed necessary to make this large heat sink accessible for the removal of the energy deposited and of the Joule heating produced during the transient. This condition can be satisfied once the CICC is designed to operate in the so called *well-cooled* regime, i.e. when the Joule heat production is lower than the heat transfer to the helium [2,20–25]. This heat balance can be expressed using the CICC material fractions and the operating current as [26]:

$$I_{op} \le \sqrt{\frac{A_{cu}^{st} w_p^{st} h (T_c - T_{op})}{\eta}}, \tag{14}$$

where h is the heat transfer coefficient from the strands to the helium, and the copper cross section and wetted perimeter are measured normal to the strand. Using their values in direction normal to the conductor and introducing the material fractions and the cable space operating current density, the limit on this last is given by:

$$J_{op} \le \cos(\theta) \sqrt{f_{cu}(f_{cu} + f_{nc}) \frac{4 K_p h (T_c - T_{op})}{\eta d}}. \tag{15}$$

Equation (15) gives the maximum allowable cable space current density for operation in the well-cooled regime. For operating current density below the value specified above, the energy margin is approximately equal to the heat capacity available in the helium. A satisfactory approximation is given by the difference of the helium enthalpy, rather than internal energy, between the operating temperature T_{op} and the current sharing temperature T_{cs}. Using the material fractions we express the stability margin per unit strand volume as:

$$\Delta E = \frac{f_{he}}{f_{cu} + f_{nc}} \rho \left[H(T_{cs}) - H(T_{op}) \right], \tag{16}$$

where H is the specific enthalpy of the helium and ρ is its density (the process is assumed to be at constant density). Although very simple, the above expression is not well suited for analytical studies of the stability margin of the cable. To study the properties of the stability margin of the cable as a function of the material fractions we can approximate again assuming that the helium enthalpy difference is given by:

$$H(T_{cs}) - H(T_{op}) \approx C_p (T_{cs} - T_{op}), \tag{17}$$

where C_p is the specific heat at constant pressure. Substitution of eq. (17) into eq. (16) and the use of the following definition for the current sharing temperature:

$$T_{cs} = T_c - \frac{J_{op}}{\cos(\theta) J_c f_{nc}} (T_c - T_{op}), \tag{18}$$

leads to a linearised form of the stability margin in terms of the material fractions in the cable space, the cable space current density and the critical properties of the superconductor:

$$\Delta E = \frac{f_{he}}{f_{cu} + f_{nc}} \left(1 - \frac{J_{op}}{\cos(\theta) J_c f_{nc}} \right) \rho C_p (T_c - T_{op}), \tag{19}$$

where J_c and T_c are respectively the critical current density (referred to the *non-copper* area) and critical temperature for the superconducting material. The expression derived above is simple enough for algebraic manipulation.

The cable ac loss and an estimate for the other energy releases can be used now to give the required energy margin at operation. From eq. (19) we can derive the maximum allowable cable space operating current density under the specified energy margin at operation ΔE:

$$J_{op} = \cos(\theta) J_c f_{nc} \left(1 - \left(\frac{1 - f_{cu} - f_{nc}}{f_{cu} + f_{nc}} \right)^{-1} \frac{\Delta E}{\rho C_p (T_c - T_{op})} \right). \tag{20}$$

The expression above represents a surface in the plane $f_{cu} - f_{nc}$ and has been plotted in fig. 3 for the choice of parameters representative of a CICC for fusion magnets application given in table 1. The surface shows some interesting properties:

(a) The operating current density J_{op} is zero when f_{nc} is zero (no superconducting material present) or when the quantity in parenthesis on the r.h.s. of eq. (20) is zero. This second condition is represented by a straight line with slope -1 and corresponds to a conductor with an amount of helium insufficient to satisfy the energy margin requirement.

(b) At constant void fraction the allowed operating current density J_{op} always *increases* when the non-copper fraction f_{nc} *increases*.

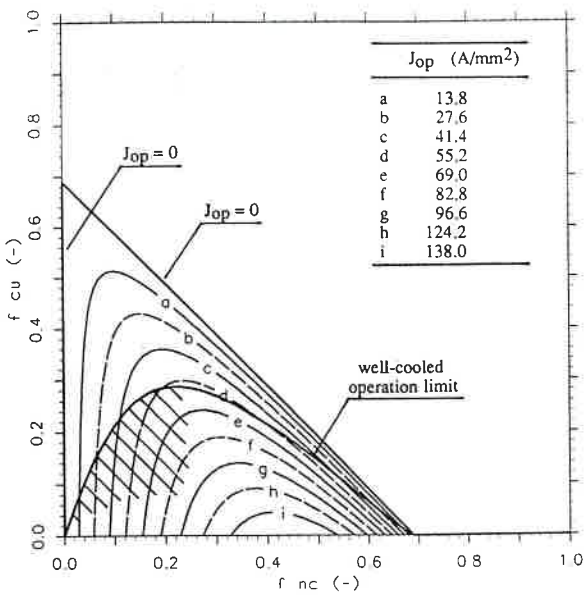

Fig. 3. Map of the allowable operating current density under a specified energy margin as computed from the linearised expression-of eq. (20) with the parameters choice of table 1. The partially shaded area below the solid curve indicates a region with copper fraction insufficient to satisfy the well-cooled operation limit of eq. (15) (see text).

Table 1
Choice of parameters for the conductor used in the examples of optimization

Conductor characteristics	
Superconducting material	Nb_3Sn
Critical current density	490 A/mm^2
Critical temperature (both at $B = 12$ (T), $T = 4.5$ (K), $\epsilon = 0.6\%$)	8.5 K
Residual Resistivity Ratio (RRR)	100
Strand diameter	0.75 mm
Void fraction	40%
Operating conditions	
Magnetic field	12 T
Helium temperature	4.5 K
Helium pressure	5 bar
Strain	-0.6%
Average heat transfer coefficient	800 W/m^{2}K
Average friction factor	0.01
Limits of operation	
Required energy margin	500 mJ/cm^3
Hot-spot temperature	150 K
Quench pressure	250 bar
Dump time constant	10 s

(c) At constant non-copper fraction f_{nc} the operating current density J_{op} always *increases* at *decreasing* copper fraction f_{cu}.

(d) At constant copper fraction f_{cu} the operating current density J_{op} has a maximum with respect to the non-copper fraction f_{nc}. An increase in J_{op} is obtained increasing f_{nc} for an initial value below the maximum and decreasing it above the maximum.

It must be kept in mind that all these properties are valid only when the copper fraction is larger than the one necessary for operation in the well-cooled regime, the condition expressed in eq. (15). This condition has been reported in fig. 3 as a lower limit on the copper fraction. Similarly, any other limitation on the copper fraction, such as the ones for protection expressed by eqs. (11) and (13), could be reported in the plane $f_{cu} - f_{nc}$, so that the search of the optimum copper and non-copper fractions could be very easy, at least graphically.

A consequence of the above properties (b) and (c) is that the optimal design in this linearised study corresponds always to the minimum copper fraction necessary to satisfy the limits, e.g. on well-cooled operation or protection. We also note that everywhere in the surface (by virtue of eq. (20)), the non-copper fraction is such that the current sharing temperature is the same, and has the value specified by the energy margin requirement.

We remember that this is only a linearised analysis, and, therefore, approximated. More reliable results could be found using the non-linear form of eq. (16) for the energy margin. However, in this case, as shown in the next section, it is possible to find a more effective optimization procedure than the one based on the surface of eq. (20).

5. Design of the optimal CICC

We start summarizing the discussion in the preceding sections, examining the freedom and limitations on the choice of the design parameters given in the introduction. In particular, several parameters or group of parameters can be set only in a restricted range due to limits on technical feasibility or manufacturing cost. This is for instance the case for the set of superconducting material, critical current density and hysteresis loss behavior. The same holds for the combination of cabling pattern, strand coating and coupling losses in the cable. We assume for simplicity that the only independent parameters (limited by the achievable

standards) are the superconducting material and the critical, non-copper current density. Hysteresis and coupling losses are assumed known. Further on, the choice of the void fraction in the cable of fig. 1 is limited in the rather tight range 35 to 45% to avoid to have a loose cable into the jacket at high void fraction or to prevent cabling damages and avoid to engage the strands too tightly in the jacket at low void fraction. The strand diameter is set by cable manufacturing and cost issues in the mm range, typically between 0.5 and 1.5 mm. Similarly, also due to manufacturing and cost problems, the copper: non-copper ratio has an upper limit, although for NbTi there is some more flexibility than for Nb_3Sn. Finally, the flow conditions must satisfy the limits on the capabilities of the cryo-plant (pressure drop, mass flow, power) and this has an impact on the values of the operating pressure, temperature and of the heat transfer coefficient.

Among all the limits to be satisfied, the one given by the stability margin is surely the most complex for the optimization. However, according to the linear optimization presented in the previous section, it is indeed possible to find the best choice of copper and non-copper fractions, two of the design parameters, satisfying all limits. For the moment we can fix the remaining parameters – critical current density, strand diameter, void fraction, flow conditions – and we select the required energy margin from the ac loss characteristics of the chosen material and mechanical energy releases. We concentrate first on the calculation of the optimal copper and non-copper fractions. This first optimization procedure is the basis for the more general optimization, including the other design parameters.

5.1. Optimal copper and non-copper fractions

We want to use non-linear helium properties for the estimate of the stability margin of the cable, as in eq. (16), and therefore the direct optimization in the $f_{cu} - f_{nc}$ plane illustrated previously is not convenient. The reason is that in this case the surface optimization requires the evaluation of the non-linear helium properties for several choices of copper and non-copper fractions. We can nevertheless assume that the properties of the optimum studied in the linear case also hold, at least approximately, in the non-linear case. In particular, in the case of a fixed void fraction the requirement on the energy margin automatically gives a requirement on the current sharing temperature (through the inversion of the $H(p, T)$ function for helium). The required margin will be achieved when the non-copper fraction is operated at a current density equal to the non-copper critical current density computed at the required current sharing temperature (and specified field). This gives the value of the optimal operating current density for the non-copper fraction:

$$J_{nc}^{opt} = J_c(T_{cs}, B).$$

Operation above this *optimal* value is not possible because the energy margin is not sufficient (lower T_{cs} than required). Below the *optimal* value the energy margin is larger than required (higher T_{cs} than required). Note that both steps involve simple non-linear calculations and do not imply any linearization of the material properties.

We recall, from the discussion on the linear case, that the optimal choice for the copper fraction is the lowest possible according to the various limits, e.g. on well-cooled operation or protection. Now it is an easy matter to find the copper fraction such that the cable space current density satisfies the limits and corresponds to the optimal, non-copper current density given by the specification on the margin. This can be done, for instance, by small steps on the copper fraction, verifying the maximum allowed operating cable space current density and checking that the corresponding non-copper current density is equal to the optimal value. The whole procedure is much more effective than the surface search because it requires the evaluation of the helium properties only once. A graphical clarification of this process is given in Fig. 4 where the maximum allowable cable space current density determined by the well-cooled and protection limits of eqs. (15), (11) and (13) is compared to the cable space current density corresponding to operation at the required current sharing temperature of 6.3 K for the choice of parameters given in table 1. The limits are represented in the figure by dashing the prohibited regions. On the left of the optimum point the copper fraction is not sufficient and the energy margin at the maximum allowed operating current density is higher than required. On the right the copper fraction is too large and the remaining non-copper fraction can operate under the required energy margin only at a current density which is below the well-cooled and protection limits.

5.2. Optimal conductor

The remaining design parameters – critical current density, strand diameter, void fraction, flow conditions

a cable-in-conduit conductor," IEEE Trans. Magn. 27 (1991) 1900–1903.
[25] L. Bottura, N. Mitchell and J. Minervini, Design criteria for stability in cable-in-conduit conductors, Cryogenics 31 (1991) 510–515.
[26] Z.J.J. Stekly and J.L. Zar, Stable superconducting coils, IEEE Trans. Nucl. Sci. 12 (1965) 367–372.
[27] N. Mitchell, L. Bottura and A. Portone, A consistent design procedure for the derivation of conceptual designs for superconducting tokamaks, NET Internal Report, N/R/3500/16/B (1991).